



Passive monitoring of particulate matter and gaseous pollutants in Fogo Island, Cape Verde



Célia A. Alves^{a,*}, Carla Candeias^{b,c}, Teresa V. Nunes^a, Mário J.C. Tomé^d, Estela D. Vicente^a, Paula F. Ávila^e, Fernando Rocha^b

^a Centre for Environmental and Marine Studies (CESAM), Department of Environment and Planning, University of Aveiro, 3810-193 Aveiro, Portugal

^b Geobiosciences, Geotechnologies and Geoengineering Research Centre (GeoBioTec), Department of Geosciences, University of Aveiro, 3810-193 Aveiro, Portugal

^c EPIUnit, Epidemiology Research Unit, National Institute of Health, R. das Taipas n°135, 4050-600 Porto, Portugal

^d School of Technology and Management, Polytechnic Institute of Viana do Castelo, Av. do Atlântico, Apart. 574, 4900-348 Viana do Castelo, Portugal

^e National Laboratory of Energy and Geology (LNEG), R. da Amieira, Apart. 1089, 4466-901 S. Mamede de Infesta, Portugal

ARTICLE INFO

Keywords:

Dust deposition
OC and EC
Ions
Morphology
Acid gases
SO₂
VOCs

ABSTRACT

An air quality monitoring campaign by passive sampling techniques was carried out, for the first time, between November 2016 and January 2017 on the Cape Verdean island of Fogo, whose volcanic mountain rises up to 2829 m. Levels of SO₂ and acid gases (HF, HCl, HNO₃, H₂SO₄ and H₃PO₄) were, in most cases, below the detection limits. Alkylpentanes, hexane, cycloalkanes and toluene were the dominant volatile organic compounds. The m,p-xylene/ethylbenzene ratios revealed that air masses arriving at Cape Verde have been subjected to significant aging processes. High toluene/benzene ratios suggested extra sources of toluene in addition to vehicle emissions. Deposition rates of total settleable dust ranged from 23 to 155 mg/m²/day. On average, organic carbon accounted for 15.6% of the dust mass, whereas elemental carbon was generally undetected. Minerals comprised the dominant mass fraction. The dust levels were mostly affected by two main airflows: the westerlies and the Saharan Air Layer. These air masses contributed to the transport of mineral dust from desert regions, secondary inorganic constituents (SO₄²⁻, NO₃⁻ and NH₄⁺) and tracers of biomass burning emissions, such as potassium. Sea salt represented 12% of the mass of settleable dust. Scanning electron microscope observations of several particles with different compositions, shapes and sizes revealed high silica mass fractions in all samples, as well as variable contents of carbonates, sulphates, aluminosilicates, Fe, Ti, F and NaCl, suggesting that, in addition to the already mentioned sources, dust is likely linked to industrial emissions in the northern and north-western coast of the African continent. Although some atmospheric constituents presented higher concentrations near the crater, the small fumarolic activity still present after cessation of the eruption in February 2015 has a limited impact on air quality, which is most affected by long range transport and some local sources at specific locations.

1. Introduction

Fogo is the island of the Sotavento group of Cape Verde that reaches the highest altitude: nearly 3000 m above sea level at its summit, Pico do Fogo. The island has an area of 476 km² and approximately 40,000 inhabitants. The economy is essentially based on agriculture and fishing. The largest city, São Filipe, is located to the west. The island is a stratovolcano that has been intermittently active. The volcanic cone rises from a plateau about 8 km in diameter, called Chã das Caldeiras, and the walls on the western side reach almost 1000 m and end in a crater 500 m in diameter and 180 m deep. After 19 years of quiescence, Fogo volcano erupted in November 2014. The eruption produced fast-

moving lava flows that travelled for several kilometres. Although the eruption of the volcano has ceased in February 2015, minor fumarolic activity is still present at the edge of the new crater. Moreover, the deposited ash is frequently remobilised by the wind causing significant health concerns. Fogo has a tropical savannah climate characterised by a relatively dry period and a wet period, the latter between August and October. Because of the altitude, temperatures are slightly lower than those of other islands of Cape Verde. The average annual temperature on the coast is roughly 23–25 °C, but decreases to values around 12–14 °C on the highest locations. There is an ever blowing, sometimes fierce sea wind on Fogo, which may temper temperatures. Nevertheless, when the dry and dusty Harmattan winds blow from the Sahara Desert

* Corresponding author.

E-mail address: celia.alves@ua.pt (C.A. Alves).

<https://doi.org/10.1016/j.atmosres.2018.08.002>

Received 24 March 2018; Received in revised form 11 July 2018; Accepted 7 August 2018

Available online 09 August 2018

0169-8095/ © 2018 Elsevier B.V. All rights reserved.

over West Africa, which frequently occurs between the end of November and the middle of March, warm air is supplied to the island and temperatures rise.

The Cape Verde archipelago does not have an air quality monitoring network. Most of the studies have been carried out at the Cape Verde Atmospheric Observatory (CVAO), in the Barlavento island of São Vicente (Fomba et al., 2013, 2014; Jenkins et al., 2013; Müller et al., 2010; Niedermeier et al., 2014; Patey et al., 2015; Sander et al., 2013; Read et al., 2012). CVAO aims to advance understanding of climatically-significant interactions between the atmospheric remote background conditions and the ocean and to provide long-term data from field campaigns. Trace gas measurements began at the site in October 2006. Chemical characterisation of aerosol measurements and flask sampling of greenhouse gases began in November 2006, halocarbon measurements in May 2007, and physical measurements of aerosol in June 2008. On-line measurements of greenhouse gases began in October 2008. A study on the aerosol composition, sources and transport was also conducted between January 2011 and January 2012 at the former airport of Praia, in the south-eastern edge of the Sotavento island of Santiago, within the CV-Dust project (Almeida-Silva et al., 2013; Fialho et al., 2014; Gama et al., 2015; Gonçalves et al., 2014; Salvador et al., 2016). All these studies provide temporal discrimination, but are limited in what concerns the coverage of geographical patterns.

To our knowledge, no atmospheric monitoring study has been conducted so far in Fogo, an island with unique characteristics. As observed in other islands of the archipelago, it is expected that emissions from the ocean and the outflow of Saharan and Sahelian dust also affect Fogo. The long range transported air masses are mixed with freshly emitted pollutants from local sources, likely including volcanic ashes and fumaroles. The objective of the current study was to obtain, by passive methods, the distribution of dust and gaseous pollutants in this tropical Atlantic marine environment, in which the complex terrain and the absence of significant anthropogenic sources makes it appropriate for evaluating remote atmospheric conditions. This information is important not only to assess cumulative exposures, but also to better understand local and transboundary sources, circulation patterns and climate implications.

2. Methodologies

2.1. Sampling and analytical techniques

Due to the lack of electricity in many places and the complex topography, a baseline air quality screening based on passive sampling, starting on November 21, 2016, was carried out at 21 locations around the island (Fig. 1). This period is representative of the long dry season, since Cape Verde's climate is consistent through the year, with only a rainy season in the early autumn months, with September providing almost half of the annual average rainfall for the islands. Thus, in this study, atmospheric particulate matter settled by gravity involved only dry processes. Settleable particulate matter was collected on 47 mm diameter quartz fibre filters (Pallflex®), which were placed in uncovered petri dishes (Analyslide® from Pall) of the same internal size. These sampling devices were positioned at a height of approximately 120 to 150 cm height above floor level to represent the breathing zone. Filter pairs were exposed side by side to dust fall for 2 months. Before sampling, the filters were conditioned for at least 24 h in a room with constant humidity (50%) and temperature (20 °C) in accordance with the European Standard EN14907:2005. After sampling, the filters were reconditioned, reweighed and stored at –18 °C until chemical analyses. The gravimetric quantification was performed with a microbalance (RADWAG 5/2Y, accuracy of 1 µg). Filter weights were obtained from the average of six consecutive measurements with variations between them of < 0.02%.

Passive sampling tubes for volatile organic compounds (VOCs), acid gases (HF, HCl, HNO₃, HBr, H₃PO₄ and H₂SO₄) and SO₂ from Gradko International Ltd. (UK) were exposed at the same sites for 3 weeks,

starting on the same date as the settleable dust. These commercial polypropylene tubes, containing a paper filter impregnated with NaHCO₃ in glycerol or a tape treated with triethanolamine, were used for collecting acid gases and SO₂, respectively. After exposure, the filters or tapes were leached in water and analysed by ion chromatography (Dionex ICS1100 ICU10), following the Gradko in-house methods GLM3 (acid gases) and GLM1 (SO₂), which were certified by the United Kingdom Accreditation System (UKAS). VOCs were sampled in stainless steel tubes packed with Tenax and then determined by thermal desorption and gas chromatography coupled to mass spectrometry in accordance with ISO16000-6.

Each filter of a pair was analysed for its carbonaceous content by a thermal-optical technique and for water soluble ions by ion chromatography. The respective pairs were investigated by scanning electron microscopy to determine the type of minerals present, their size and shape.

For analysis of the carbonaceous material, two 9 mm diameter filter punches were used in each analytical run. Two replicate analyses for each sample were performed, one with acidification of the filter, the other without acidification. The difference between both determinations provides a rough estimate of the carbonate content. The filter punches were first heated in a non-oxidising atmosphere of N₂ in order to volatilise the carbonaceous organic compounds (organic carbon, OC). After the first step of controlled heating, the remaining fraction was burnt in an oxidising atmosphere (mixture of N₂ and O₂) to evolve elemental carbon (EC). The CO₂ resulting from the thermal desorption/oxidation of particulate carbon was quantified by a non-dispersive infrared (NDIR) analyser. During the anoxic heating, some OC is pyrolysed (PC), and for that reason, it is quantified as EC in the second stage of heating. The interference between PC and EC can be controlled by continuous monitoring of the blackening of the filter using a laser beam and a photodetector measuring light transmittance. Each one of the replicates was previously acidified in order to evaluate the influence of carbonates in the quantification of EC and OC. Punches of the filters were exposed to vapours of hydrochloric acid (HCl - 6 M) for approximately 4 h. After this period, the samples were transferred to a desiccator containing sodium hydroxide (NaOH), where they were kept overnight. The purpose of this process was to neutralise any excess of acid in the sample to protect the CO₂ analyser from corrosive HCl fumes.

Two other 9 mm diameter filter punches were subjected to extraction with 6 mL of Milli-Q ultrapure water under ultra-sonication for 15 min at room temperature. The liquid extracts were then filtered with a 0.45 µm pore PTFE syringe filter to remove insoluble particles, and analysed for water-soluble ions. A Thermo Scientific™ Dionex™ ICS-5000+ capillary high-performance ion chromatographic system with a dual pump was used. It enables the simultaneous determination of anions and cations in a single run.

The other filter of each pair was analysed with a HITACHI SU-70 high resolution scanning electron microscope (SEM) equipped with a Bruker energy dispersive spectroscopy (EDS) detector in order to detect the chemical elemental composition of the dust particles individually. The size and shape of each speck was also taken into consideration. The chemical analyses were interpreted in terms of particle classes (e.g. Si rich, S rich) and grossly comparable to mineralogical groups (e.g. quartz, volcanic glass, sulphates) (Scheuven and Kandler, 2014). One of the aims of this study was to investigate the possible risk of the dust particles to the individuals living at each sampling site. For this reason, the highest concentration of each element was selected. Around 30 particles in each filter were analysed by SEM/EDS. The possible secondary emission influence of Si rich phases (fibres and basaltic glass) when this EDS spectra were examined was taken into account, as well as results from the standardless analysis.

2.2. Ancillary tools

A GPS (global positioning system) was used to record the coordinates of every sampling station for later data mapping. The

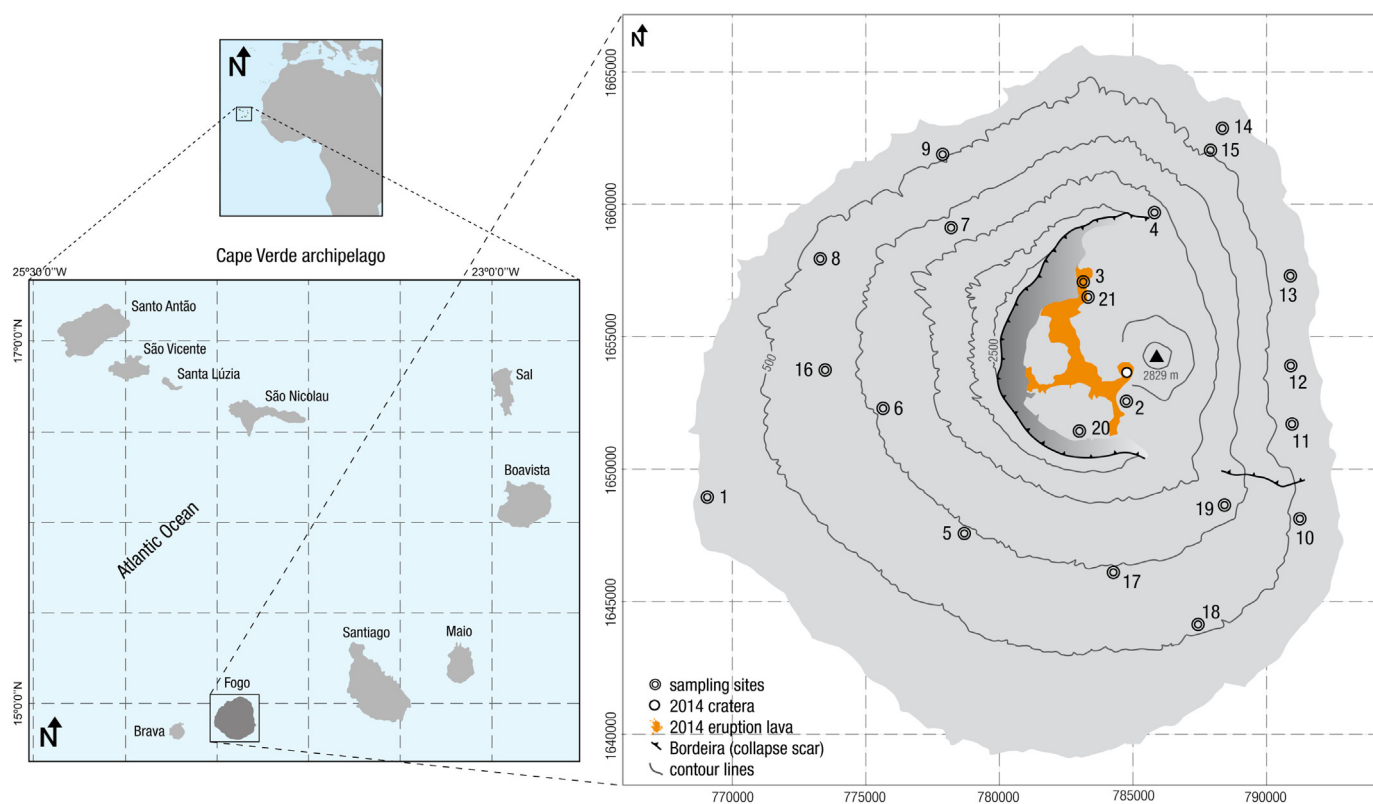


Fig. 1. Map of the archipelago and location of the sampling sites: 1 - S. Filipe, 2 - Monte Lantico, 3 - Portela, 4 - Fernão Gomes, 5 - Monte Grande, 6 - Cisterno, 7 - Monte Preto, 8 - Ponta Verde, 9 - Campanas de Baixo, 10 - Cova Figueira, 11 - Tinteira, 12 - Baleia (Pedreira), 13 - Relva, 14 - Mosteiros, 15 - Cutelo Alto, 16 - Pico Lopes, 17 - Achada Furna, 18 - Dacabalaio, 19 - Estância Roque, 20 - Cova Tina, 21 - Portela.

distributions of pollutant concentrations or sedimentation rates were drawn by the Surfer 8.0 software in which the data were plotted using the kriging gridding method. The Hybrid Single-Particle Lagrangian Integrated Trajectory model (HYSPLIT), developed by the U.S. National Oceanic and Atmospheric Administration (NOAA), was run with the National Centre for Environmental Prediction's (NCEP) Global Data Assimilation System (GDAS, 1°) data set (Draxler and Hess, 1998; Draxler and Rolph, 2003; Stein et al., 2015). Daily backward trajectories were computed at 00:00, 06:00, 12:00 and 18:00 UTC, with a run time of 240 h and an arrival height of 500 and 3000 m above ground level. These values represent approximately the average altitude at which a large part of the population lives and the highest elevation of the island, respectively. A k-means cluster analysis for the two months of sampling was performed to group air mass back trajectories into similar groups, each one representing a typical meteorological scenario. The optimum number of clusters to be retained was decided according to the percentage change in within-cluster variance as a function of the number of clusters. Hourly wind direction and wind speed data for the island (Geoname-ID: 3374613; 14.94°N, 24.39°W, 2355 m a.s.l.) were downloaded from the Meteoblue archives (<https://www.meteoblue.com>), a meteorological service created at the University of Basel, Switzerland, in cooperation with NOAA and NCEP. The wind rose for the study period was plotted using Hydrognomon, a freeware developed by the National Technical University of Athens.

3. Results and discussion

3.1. Settleable particulate matter

According to a technical guidance document on monitoring of particulate matter by the UK Environmental Agency (EA, 2013), no statutory or official air quality criterion for dust annoyance has been set at European or WHO level. Also, there are no Cape Verdean standards

for dust deposition. Clark (2013) refers nuisance dust deposition limit values from nine countries, ranging from 100 mg/m²/day in New York State, USA, to 333 mg/m²/day in Finland. Dust deposition in Fogo Island ranged from 23 to 155, averaging 51 mg/m²/day (Fig. 2). The highest deposition rates were observed in the vicinity of the crater, where values fell in the range of dustfall limits reported by Clark (2013) for different countries. For other locations on the island, the particulate matter dry deposition rates were lower than 100 mg/m²/day and therefore cannot be classified as nuisance dusts. Higher deposition rates of total settleable dust (70–700 mg/m²/day) were monitored at background mountainous areas in northeastern Chalkidiki, Greece (Gaidajis, 2002). During a dust storm that hit the Al-Ahsa Oasis of Saudi Arabia astonishing deposition rates of 2.84 ± 1.2 g/m²/day were registered (Almuhanna, 2015). Average dust deposition rates ranging from 0.137 mg/m²/day in Penny Ice Cap (Canada) to 1233 mg/m²/day in desert regions of China have been reported in a recent review paper (Amodio et al., 2014). Particulate matter dry deposition rates varying from 0.3 to 105.8 (average = 23.6) mg/m²/day were obtained in Sierra Nevada, a remote mountain site located in the south of the Iberian Peninsula, close to the Mediterranean Sea (< 25 km), far from direct human activity, but highly influenced by Saharan dust intrusions (Morales-Baquero et al., 2013).

It has been reported that, between December and February, atmospheric particulate matter levels in Cape Verde are prompted by the advections of African dust (Gama et al., 2015; Salvador et al., 2016). Dust particles are transported in the so-called Saharan Air Layer (SAL), the warm, dry and dusty airstream that expands from North Africa to the Americas at tropical and subtropical latitudes. Furthermore, aerosols emitted in the boundary layer of North America are regularly exported to the North Atlantic free troposphere, where they experience transatlantic transport in the westerlies. It has been observed that the westerly jet and the associated eastward moving cyclones contribute to non-sea-salt-sulphate, nitrate and ammonium aerosol loads at Izaña

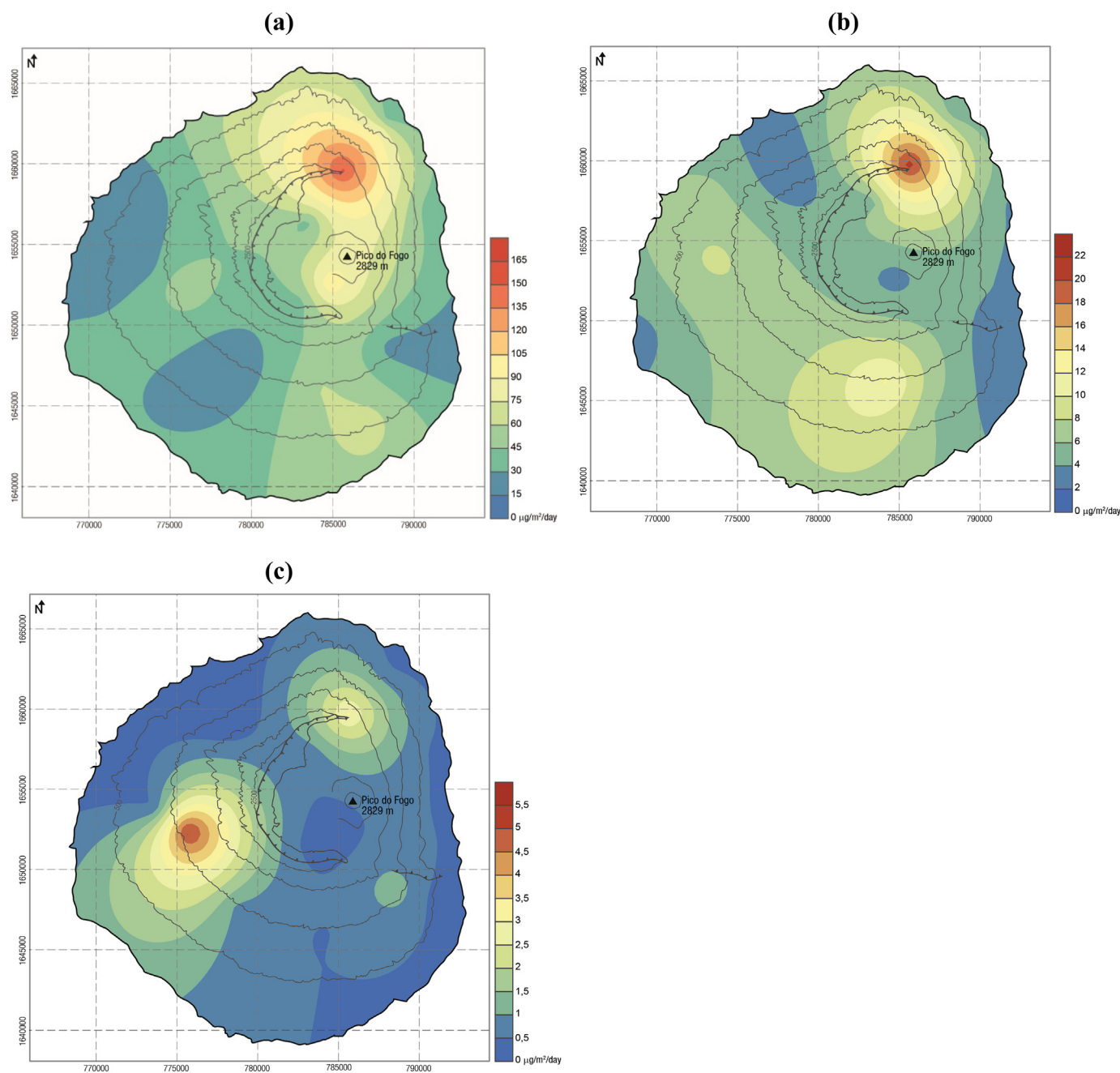


Fig. 2. Deposition rates of total settleable particulate matter (a), organic (b) and elemental carbon (c).

Global Atmospheric Watch Observatory at 2367 m.a.s.l. in Tenerife, Canary Islands (García et al., 2017). This prevailing airstream that flows across the North Atlantic at subtropical and mid-latitudes exports polluted air from Northeastern United States, where the highest SO_2 emissions occur. Moreover, dust emissions in a region that expands from SW Texas northward throughout the High Plains, and subsequent export to the Atlantic, may also affect the aerosol loads and composition in the archipelagos along the African coast. The High Plains are among the major dust sources in North America. It has been pointed out that conversion of land from natural vegetation to agriculture or pasturage could adversely affect surface levels of mineral dust by modifying surface sediments and soil moisture; as a result, the frequency and amount of airborne dust increase (García et al., 2017; and references therein).

The possibility that these two main airflows (westerlies and SAL) affect Cape Verde was tracked by means of backward trajectory

analysis. Six trajectory clusters were found (Fig. 3). The most frequent air flows reaching the lowest height (500 m) were those represented by clusters 1 and 3, grouping 49% of the total number of trajectories. These clusters gather fast easterly and north-easterly trajectories of air masses, respectively, coming from the African mainland or crossing the coastal line of Morocco, Western Sahara, Mauritania and Senegal. The main potential source areas in the northern border line of Morocco and Algeria include oil and coal power plants, crude oil refineries and fertiliser industries, among others (Rodríguez et al., 2011; Salvador et al., 2016), contributing to the mixing of dust with anthropogenic aerosols. Cluster 1 represents the transport of dust plumes originated in south Sahara and Sahelian regions. Cluster 2 (30% of the total number of trajectories) was constituted by regional north-easterly atmospheric circulations over the Cape Verde archipelago, which prevailed over advective air mass flows. The occurrence of north-westerly trajectories, which were grouped into clusters 4–6 (21% of the total number of

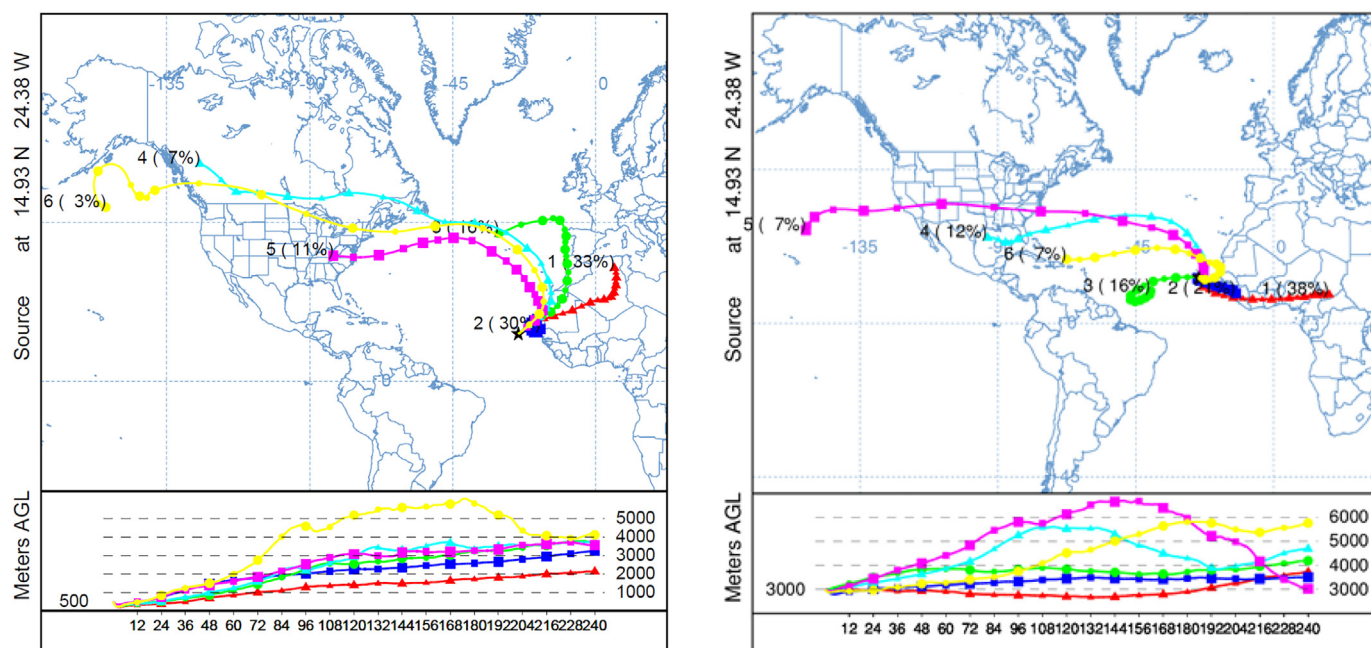


Fig. 3. HYSPLIT clusters of backward air trajectories arriving at 500 and 3000 m. Coloured lines represent the mean trajectory of each cluster. Clusters are numbered and values in parentheses represent the percentage of backward air trajectories included in each cluster.

trajectories), was also observed. For the arrival height of 3000 m, the air masses coming from North America are more displaced to the south. The dominant cluster (38%) is the one that groups trajectories originated between the Sahel and the equatorial region. The influence of air masses from North Africa is lost, while the Atlantic influence gains visibility.

In the present study, most of the total mass of particulate matter was usually made up of mineral material, whereas carbonaceous constituents represented a less important fraction. A low carbonaceous content in atmospheric particulate matter with aerodynamic diameter lower than $10\ \mu\text{m}$ (PM_{10}) collected over a 1-year long campaign in Praia City, Santiago Island, was also documented by Gonçalves et al. (2014). In Santiago, OC and EC represented, on average, 1.8% and 0.41% of the aerosol mass, respectively, suggesting that most of it was of mineral origin. OC sedimentation rates in Fogo ranged from 2.1 to 21.1 $\text{mg}/\text{m}^2/\text{day}$ (average = 6.3 $\text{mg}/\text{m}^2/\text{day}$), accounting for 3.1–52.9% of the dust mass (average = 15.6%). The highest OC sedimentation rate was observed in an uninhabited agricultural location near the crater at 1900 m (Fernão Gomes), where the maximum dustfall value was also registered (Fig. 2). However, the OC mass fraction (13.8%) in settleable particulate matter for this sampling site was close to the average for the whole island. During the eruption of 2014, the settlements of Portela and Bangaieira, located within the caldera, 4–5 km NW of Pico, were destroyed by lava flows, which reached the boundaries of Fernão Gomes. An extensive agricultural area was flooded by the lava, including a vast area used for agriculture, such as fruits, wine, vegetables, and coffee plantations. For most places, EC accounted for < 1% by weight. Higher particulate matter mass fractions were observed in samples collected at Fernão Gomes (2.0%), S. Filipe (3.4%), Monte Grande (6.3%), Cisterno (9.3%), Pico Lopes (2.4%) and Estância Roque (5.1%). Following the 2014 eruption, intense ashfall was reported for the latter place, which is situated on the flanks of the volcano. Monte Grande is a settlement in the central part of the island, located at about 900 m in elevation, 10 km east of the island capital São Filipe, where part of the evacuated caldera communities was relocated following the last eruption. Besides the additional human activities that followed the eruption, traffic emissions may also contribute to the carbon levels observed in Monte Grande. The village is linked by roads with other main settlements, bypassing S. Filipe, including a route connected to the circular road that has access

to the capital. Pico Lopes is a small village where bonfires are often detected, lasting for several hours, which may contribute to the relatively high EC particulate matter mass fraction. Cisterno is also a small village located at 900 m altitude in the western part of the island. Relevant local EC emission sources are unknown at this place. It should, however, be taken into account that the small village is bordered by a triangle of roads (EN3-FG-01, EN3-FG-06 and EM-SF-12).

Carbonate carbon was roughly inferred from the slope of the regression line between total carbon (OC + EC) in acidified filters and total carbon in non-acidified filters (Fig. S1). It was observed that CO_3^{2-} represented < 3% of total carbon, which corresponds, on average, to about 0.5% of the mass of settleable dust. Salvador et al. (2016) reported a PM_{10} mass fraction of 1.4% for this carbonaceous component in samples collected in the surroundings of Praia City at Santiago Island between January 2011 and January 2012. Since it is known that the northern and western Sahara lies upon a carbonated lithology, and taking into account that the long-range transport from these regions is relatively frequent, a higher carbonate content would be expected. Calcium carbonate is considered as the most chemically reactive mineral component in aeolian dust particles (e.g. Laskin et al., 2005). Its strong alkaline nature causes it to react promptly with acidic gases, such as HNO_3 , HCl , and SO_2 , leading to the formation of the respective salts (calcium nitrate, calcium chloride, and calcium sulphate). The conversion of insoluble calcium carbonate particles to deliquescent calcium nitrate through reaction with HNO_3 was first observed in laboratory experiments (Krueger et al., 2004) and has also been further confirmed in field studies (Laskin et al., 2005; Shi et al., 2008; Sullivan et al., 2009). Low carbonate carbon contents are also consistent with contributions from suspension of surface soils depleted of calcium carbonate by weathering. The abundance of carbonate carbon is influenced by the presence of precipitation, as well as the underlying formation in the region (Chow and Watson, 2002). Volcanic soils and ashes, such as those in Fogo Island, are very acidic, providing favourable conditions for carbonate weathering.

On average, the sum of water soluble ions represented 18% of the mass of settleable dust. The mean contribution of Na^+ , SO_4^{2-} , Ca^{2+} , Cl^- and NO_3^- (the major water-soluble components) to the total mass of settleable dust was 6.2, 4.8, 3.6, 2.3 and 0.65%, respectively (Table 1). These five constituents accounted for 23.4, 22.7, 16.1, 14.9

Table 1
Deposition rates of some water-soluble ions (mg/m²/day).

	F ⁻	Cl ⁻	NO ₂ ⁻	Br ⁻	SO ₄ ²⁻	NO ₃ ⁻
Min	< DL	< DL	< DL	< DL	< DL	< DL
Max	0.75	4.57	0.05	0.04	10.21	0.95
Avg	0.17	0.86	0.01	0.01	1.92	0.24
	PO ₄ ³⁻	Na ⁺	NH ₄ ⁺	Mg ²⁺	K ⁺	Ca ²⁺
Min	< DL	< DL	< DL	< DL	< DL	0.02
Max	1.09	8.59	0.31	0.47	0.95	3.62
Avg	0.21	2.10	0.14	0.09	0.27	0.91

DL – detection limit.

and 7.0% of the total mass of ions analysed, correspondingly. Although minor, still appreciable mass fractions were measured for K⁺ (0.7%), NH₄⁺ (0.4%) and Mg²⁺ (0.23%). The equivalent ratio of cations to anions is a good indicator of the acidity of the particulate matter. Based on the measurements, this ratio was, on average, close to 1.7. The presence of organic anions (oxalates and other short-chain organic acids), and compounds produced by phytoplankton activity in the sea (as MSA, methanesulfonic acid), which were not measured in the present study, may explain the deficit of negative species (Kerminen et al., 2001). For the sampling campaign carried out in Praia City, Salvador et al. (2016) reported the following percentage PM₁₀ mass fractions: Cl⁻ 9.0, Na⁺ 6.8, SO₄²⁻ 3.2, NO₃⁻ 2.0, Ca²⁺ 1.4, Mg²⁺ 0.65, NH₄⁺ 0.36 and K⁺ 0.0004. It must be borne in mind that these researchers carried out daily PM₁₀ sampling over 1-year in a single location, while the present study refers to total settleable dust over 2 months at multiple sites. Salvador et al. (2016) showed that some components associated with secondary inorganic compounds (SO₄²⁻, NO₃⁻ and NH₄⁺) increased when Saharan dust blows over the Atlantic. Rodríguez et al. (2011) also demonstrated that dust is very often mixed with North African industrial pollutants and exported to the Canary Islands in the SAL. Furthermore, as observed in Tenerife, Canary Islands, it is likely that secondary inorganic compounds observed in Fogo are also associated with one transport pathway from North-eastern USA at ~40°N and another route linked to the North American outflow by Canada and subsequent transatlantic transport at high latitudes and circulation around the Azores High (García et al., 2017). However, a study involving temporal variability in concentrations and chemical speciation of settleable dust, combined with high resolution backward air trajectories, would be needed to draw firm conclusions.

The NO₃⁻/SO₄²⁻ mass ratio has been used to identify the relative contributions to the atmospheric particulate matter from mobile versus stationary sources. The low mean ratio obtained in Fogo (0.3) could be ascribed to the predominance of long-range transport of emissions from stationary sources over pollution from mobile sources. This ratio is in the range of values reported for Chinese cities where coal combustion is the dominant source (Cao et al., 2009). NO₃⁻/SO₄²⁻ mass ratios varying from 2 to 5 were obtained by Kim et al. (2000) in downtown Los Angeles and in Rubidoux in Southern California, USA, where traffic is the main emitter of air pollutants.

Sea salt can be estimated as $1.47 \times \text{Na}^+ + \text{Cl}^-$, where 1.47 is the seawater ratio of $(\text{Na}^+ + \text{K}^+ + \text{Mg}^{2+} + \text{Ca}^{2+} + \text{SO}_4^{2-} + \text{HCO}_3^-) / \text{Na}^+$ (Quinn et al., 2002). This approach prevents the inclusion of non-sea-salt K⁺, Mg²⁺, Ca²⁺, SO₄²⁻ and HCO₃⁻ in the sea-salt mass and allows for the loss of Cl⁻ mass through depletion processes. It also assumes that all measured Na⁺ and Cl⁻ are derived from seawater. Sea salt sedimentation rates ranged from 0.30 to 27.6, averaging 3.94 mg/m²/day. This represented 12% of the mass of settleable dust. It has been observed that sea salt concentrations in PM₁₀ collected at the CVAO strongly depended on meteorological conditions and sampling height (Fomba et al., 2014). During days with high wind speeds the sea salt concentrations increased strongly, in this observatory. The highest wind

speeds were frequently registered during the westerlies. Increases in sea salt concentrations were experienced during days of high wind speeds, but a strong correlation between sea salt and the local wind speed was not observed. Sea salt and other sea-spray-associated aerosol components also increased enormously at a lower height, due to the fact that sampling was conducted within the internal marine boundary layer. In the current study, no clear pattern was observed between sea salt dry deposition rates and wind speed or altitude. It should be noted that, during the sampling campaign, calm winds (< 2 m/s) were recorded for 50% of the time (Fig. S2). A mean Cl⁻/Na⁺ equivalent ratio of 0.74 was obtained. Both ions are the major inorganic components of sea salt, but are also abundant in evaporitic lake deposits, where they are found as mineral halite. The ratio was 2.4 times lower than that in seawater (Cl⁻/Na⁺ = 1.8). Reduction is frequently observed in anthropogenically disturbed marine environments, with enhanced acidity, because of the volatilisation of HCl from NaCl crystals that had reacted with nitric and sulphuric acid (HNO₃ and H₂SO₄) to form NaNO₃ or (Na)₂SO₄ (Formenti et al., 2003). Despite the good correlation ($r^2 = 0.82$) between Na⁺ and SO₄²⁻, this hypothesis is unlikely for Fogo island, because the ionic balance is characterised by an excess of cations, especially Ca²⁺. Likewise, deposition of gaseous HCl on dust particles is discarded. The low Cl⁻/Na⁺ ratio is probably due to an additional non-evaporite dust source for Na⁺ (Formenti et al., 2003).

The strong correlation for the relationship between Mg²⁺ and Ca²⁺ ($r^2 = 0.81$) suggests they have a common source, most likely local soil or dust transported from the desert during storms. In addition to dust, sea salt is also a source of Mg²⁺. However, the very weak relationship ($r^2 = 0.15$) between Mg²⁺ and Na⁺ and a mean Mg²⁺/Na⁺ equivalent ratio of 0.26, which departs from the typical value of 0.12 of sea water, suggests that the contribution of the dust source to Mg²⁺ was larger than that of sea salt. A moderate correlation ($r^2 = 0.57$) between Ca²⁺ and NO₃⁻ was also found. The coexistence of these two ions indicates the presence of deliquescent Ca(NO₃)₂, which is formed by reaction between CaCO₃ and HNO₃ on the Ca-rich dust particles (Pan et al., 2017).

Non-sea salt potassium [$_{\text{Nss}}\text{K}^+ = \text{K}^+ - (0.0355 \times \text{Na}^+)$, where 0.0355 is the K⁺/Na⁺ ratio in seawater] was found to represent, on average, 82% of total K⁺. Sedimentation rates ranged from values around 60–90 μg/m²/day at locations such as Ponta Verde, Monte Grande, Cutelo Alto, Cova Tina, Campanas de Baixo and Monte Lantico to 600–800 μg/m²/day in Portela, Pico Lopes, Cisterno and Mosteiros. Water soluble potassium has been pointed out as a major constituent of biomass burning particles (e.g. Alves et al., 2011; Calvo et al., 2013). In addition to local biomass burning sources, it is expected that Fogo is also affected by long range transport. Every year huge amounts of aerosols are produced from wild- and agricultural fires in Africa. From October to March the most intense fires are registered in sub-Saharan west Africa (N'Datchoh et al., 2015). Global fire maps from NASA confirm the occurrence of hundreds of active events during the sampling campaign (Fig. S3).

3.2. Chemical and morphological properties of dust by SEM-EDS

The relative order of concentrations of elements with crustal origin in settled dust samples was Si > Al > Ca > Na > Mg > K > Fe > Ti > P. Among these, Si was always present, regardless of the sample, although in varying concentrations. These elements were selected since they are used as fingerprints of the Saharan/Sahel dusts by several authors (e.g. Chiapello et al., 1997; Formenti et al., 2001; Molinaroli et al., 1999; Scheuven et al., 2013). Pearson correlations disclosed significant results at the 0.05 level for the sets S/Mg (0.556), S/P (0.452), Fe/Ti (0.509) and at the 0.01 level for the pairs Si/Ca (0.580), Fe/K (0.592), Fe/Na (0.592), K/Na (1.000). According to previous studies, Si is the most abundant element in dusts, mainly in quartz (SiO₂). Mostly present in aluminosilicates and different clay minerals (e.g. illite, kaolinite, smectite), Al is the second most abundant. It

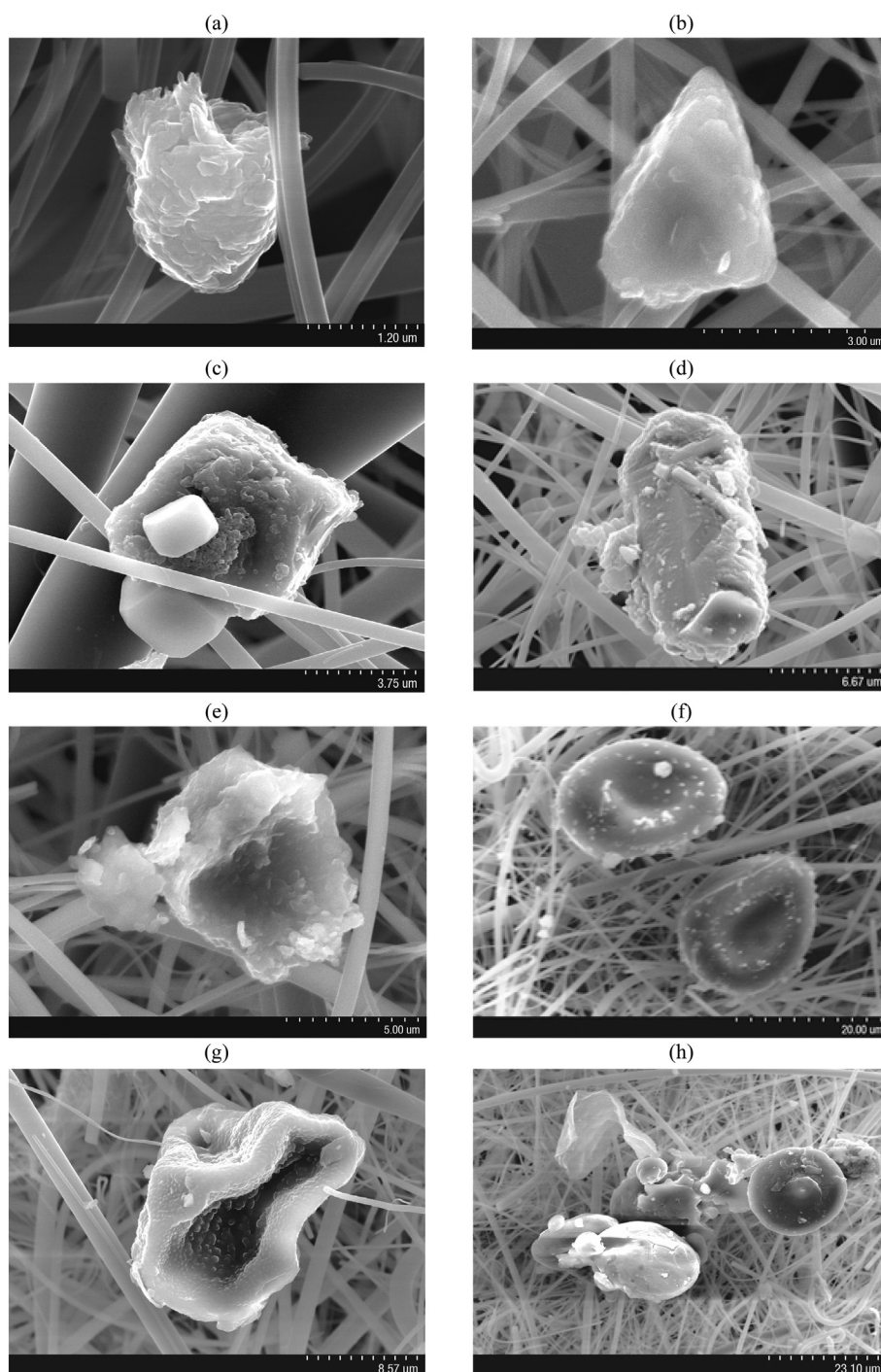


Fig. 4. SEM images: (a) Si-rich (quartz?); (b) basaltic glass; (c) plagioclase (bigger particle) and two specks of sea salts; (d) calcic Ti-bearing amphibole; (e) illite; (f) organic particle; (g) organic speck Si-rich, (h) mixture of organic particle with Na cape (right), speck with composition typical of pollution (centre) and a F-rich unit (down left). Settleable dust collected passively on quartz filters at sampling sites 11, 3, 1, 1, 3, 4, 6, and 5, respectively.

is considered a characteristic crustal marker in dusts, accounting for mass fractions of 2–8 wt% in Saharan mineral aerosol. Ca is used as a carbonate content tracer, representing > 5 wt% in Saharan dust. Na is mostly found in albitic plagioclase and in the smectite group. Mg can be traced mainly in chlorite and palygoskite, carbonates and clay minerals, while K is present in many aluminosilicates, but can also derive from biomass burning. Fe exists mostly in the form of iron oxides and hydroxides, chlorite and palygoskite. Ti is probably reflecting the presence of TiO_2 phases. P is linked to phosphate deposits and to mines existing in North Africa (Formenti et al., 2001; Scheuven et al., 2013).

The SEM analyses detected a mixture of specks with diverse sources, composition, shapes and sizes, often in agglomerates, which were very rich in < 10 μm particles. Most of the particles revealed a Si rich content, mainly quartz and basaltic glass (Fig. 4(a) and (b)). The submicron rounded quartz speck is indicative of abrasion and long-distance transport, while the PM_{10} volcanic glass presents angular edges typical of volcanic environments. Samples of settleable dust also have different carbonates, sulphates and aluminosilicates, sodium chloride, Fe-bearing, Ti-bearing, and F-bearing particles, which are suggestive of different sources: (a) volcanic environment or, (b) Saharan dusts transported to

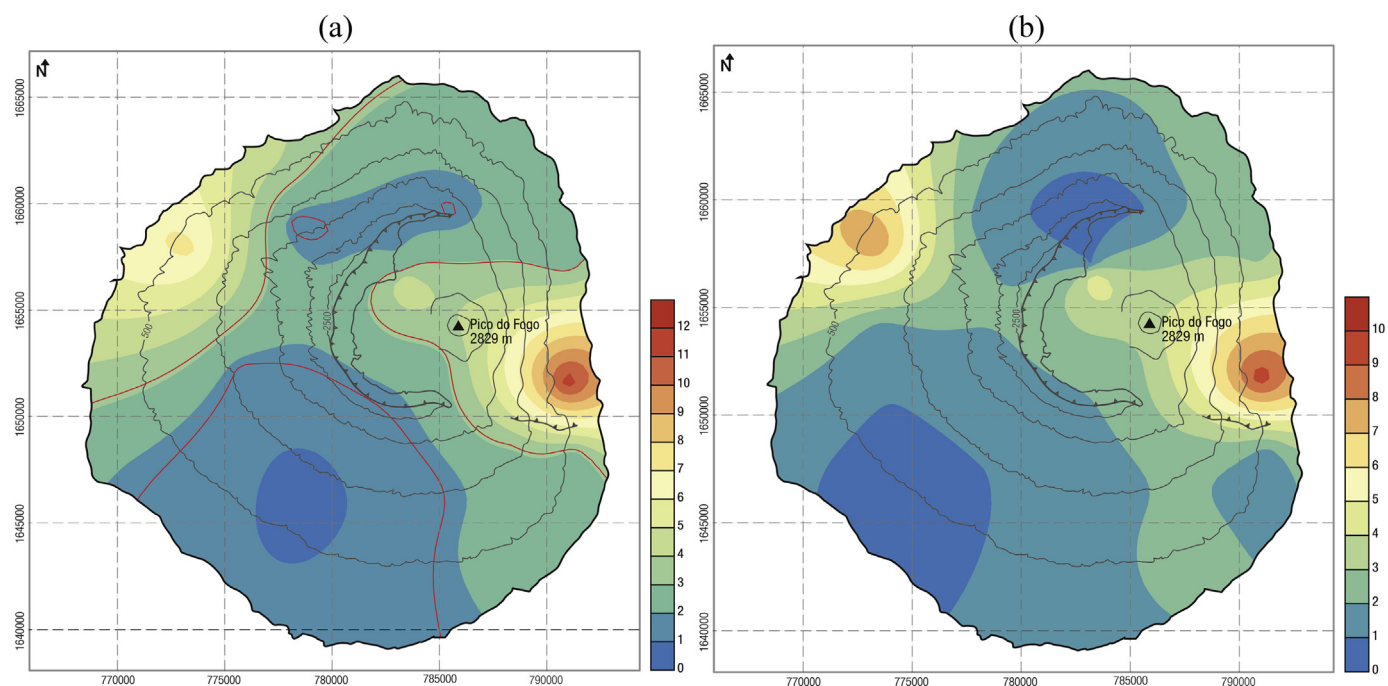


Fig. 5. Distribution of (a) Si/Al and (b) Ca/Al ratios. The red line in (a) represents the limits of the mineral dust contribution with origin in Sahara and Sahel, proposed by Chiapello et al. (1997).

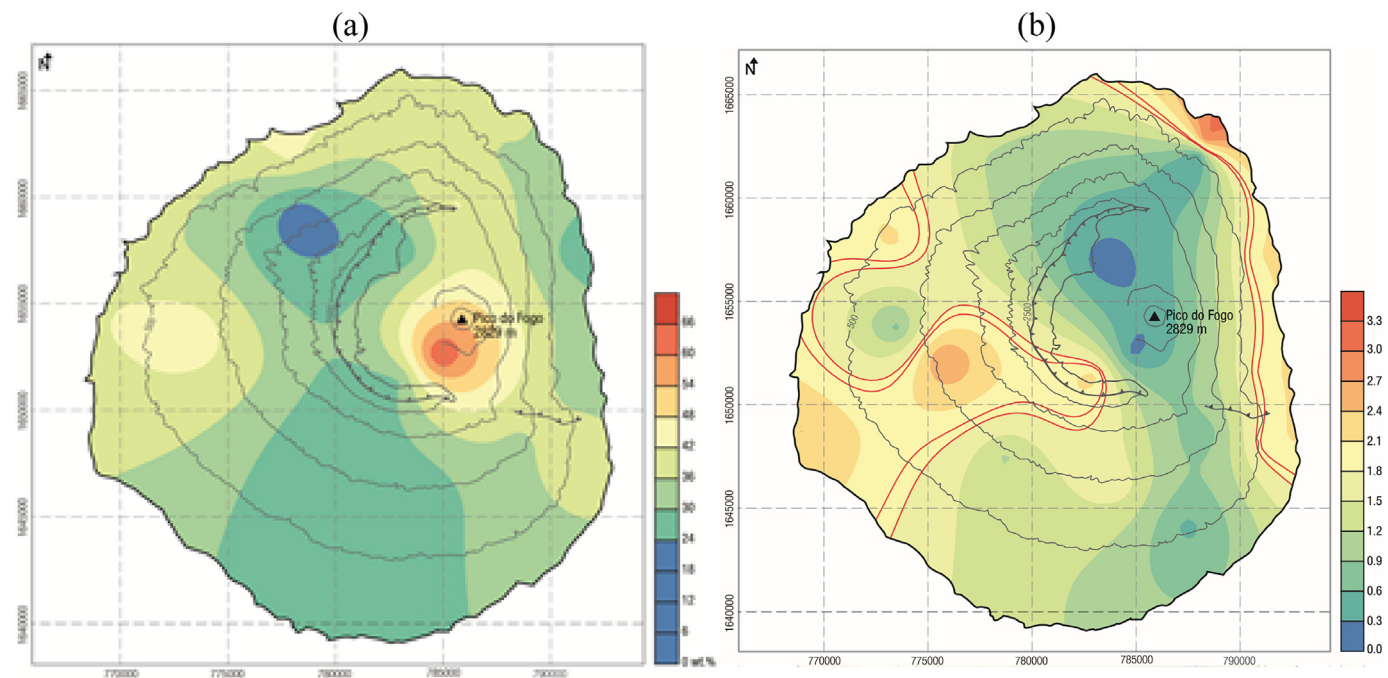


Fig. 6. Distribution of (a) Si maximum wt% concentrations, and (b) Cl/Na ratio with the red line that embodies the limits of the presence of sea salts, proposed by Riley and Chester (1971). (For interpretation of the references to colour in this figure legend, the reader is referred to the web version of this article.)

this region, (c) sea salts, (d) organic compounds, (e) pollution (biomass burning and/or urban emissions), and/or (f) a mixture of the previous. Minor amounts of S-bearing, Cl-bearing and carbonaceous specks were found (Fig. 4). The diameter of typical Saharan mineral dust that reaches Cape Verde ranges between 1 and 10 μm (Haywood et al., 2003; Weinzierl et al., 2011). Most of the particles after 1000 km or a few days of transport are < 3 μm (Scheuvs and Kandler, 2014).

Saharan and Sahelian mineral dusts can be traced by the Si/Al ratio of 2.4 ± 0.7 , proposed by Chiapello et al. (1997). The spatial distribution of this ratio (Fig. 5a) clearly reveals the effect of the mineral dusts

that are transported by the NE winds and the influence of the Pico do Fogo Mountain and the Bordeira Scar. The Ca content, and particularly the Ca/Al ratio (Fig. 5b), are also used as a compositional characteristic of the northern African dusts. Both ratios show a very similar behaviour. The dusts transported from North Africa are mostly composed of light particles of quartz [SiO_2], calcite [CaCO_3], dolomite [$\text{CaMg}(\text{CO}_3)_2$], feldspars [KAlSi_3O_8 - $\text{NaAlSi}_3\text{O}_8$ - $\text{CaAl}_2\text{Si}_2\text{O}_8$], clay minerals, such as illite [$(\text{KH}_3\text{O})(\text{Al},\text{Mg},\text{Fe})_2(\text{Si},\text{Al})_4\text{O}_{10}$], kaolinite [$\text{Al}_2\text{Si}_2\text{O}_5(\text{OH})_4$] and smectite, specifically montmorillonite [$(\text{Na},\text{Ca})_{0.33}(\text{Al},\text{Mg})_2(\text{Si}_4\text{O}_{10})(\text{OH})_2 \cdot n\text{H}_2\text{O}$], and palygorskite [$(\text{Mg},\text{Al})_5(\text{Si},\text{Al})_8\text{O}_{20}(\text{OH})_{2.8}\text{H}_2\text{O}$]

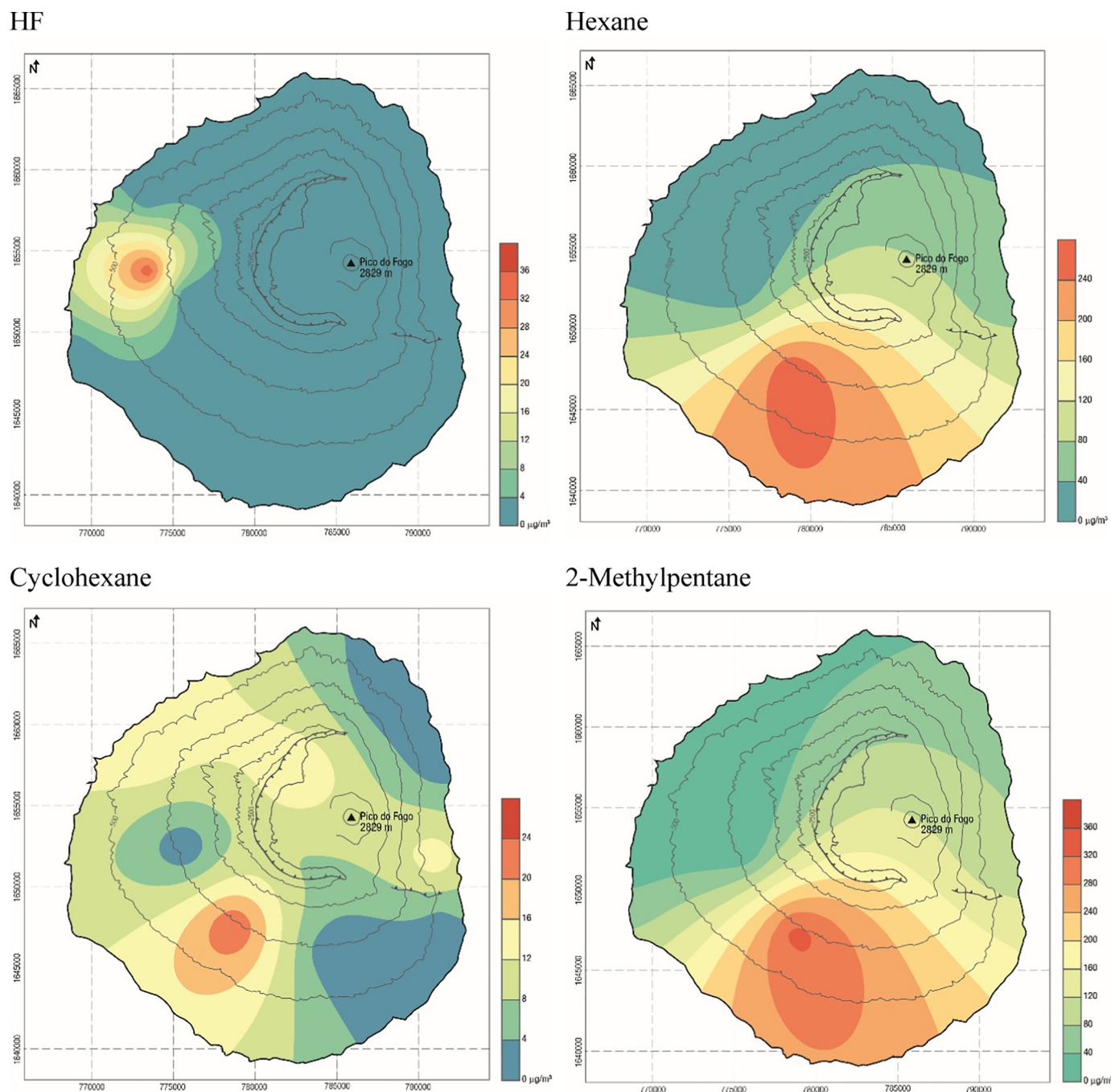


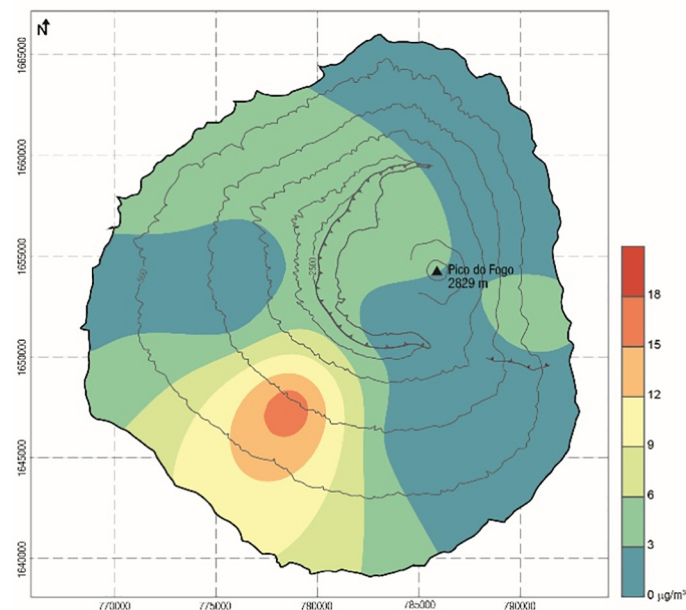
Fig. 7. Concentrations of some gaseous compounds.

(Brooks et al., 2005; Molinaroli, 1996; Remoundaki et al., 2011). Nevertheless, the distribution of Si maximum concentrations reflects the importance of the Fogo volcano vents, still active. Riley and Chester (1971) suggested that the presence of sea salts might be traced by a Cl/Na ratio of 1.84 ± 0.05 . The distribution map of this ratio (Fig. 6a) suggests the presence of salts in the lower areas of the island. The occurrence on the island of variable concentrations (0 to 34.85%) of Zn, As, Mn, Cu, Ni, Cd, and Pb, at levels estimated for urban areas (Remoundaki et al., 2011; Terzi et al., 2010), is attributed to anthropogenic sources, such as biomass and waste burning, fossil fuel and residual oil combustion, vehicle exhaust and tyre and brake wear, whether from local origin or also from transport of polluted air masses.

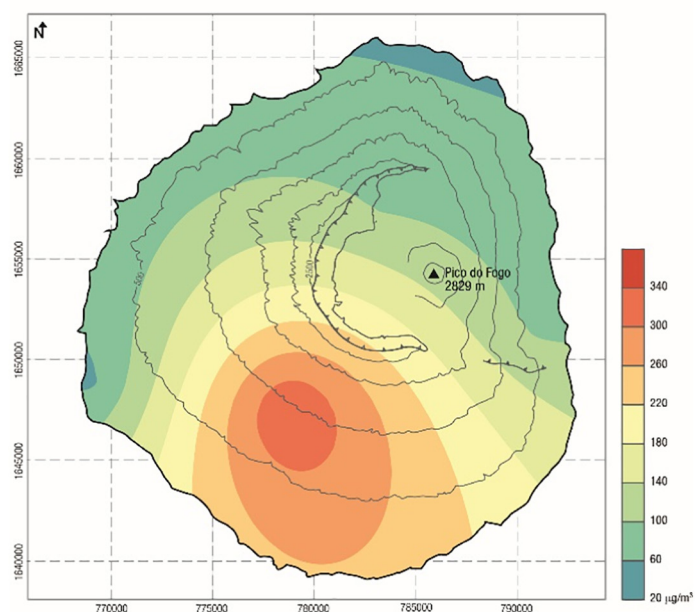
3.3. Gaseous compounds

Levels of acid gases were, in most cases, below the detection limits. The only exception was observed at a place (Pico Lopes, location 16) where traditional pig slaughter is regularly performed for the commercial distribution of meat within the island. To clean the hair off the pig, each animal is burned with oil or similar combustion fuels. The slaughter is followed by barbecue and preparation of crispy fried pork greaves. The bonfire is lit with dry acacia leaves, plastics and cardboards, and then the embers are fed with acacia logs. These practices last a minimum of 10 h a day and have possibly contributed to the high levels registered at this location: 36, 427, 15, 101 and $11 \mu\text{g}/\text{m}^3$ for HF, HCl, HNO_3 , H_2SO_4 and H_3PO_4 , respectively. In general, concentrations

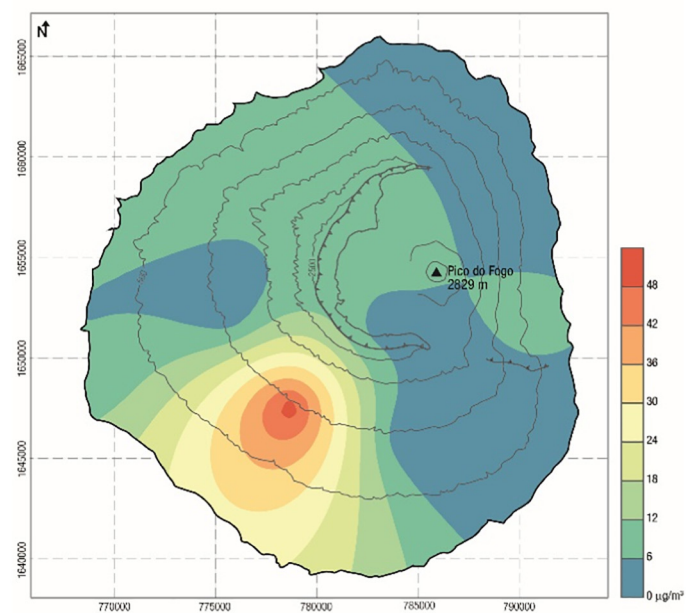
2,2-Dimethylpentane



3-Methylpentane



2,4-Dimethylpentane



Toluene

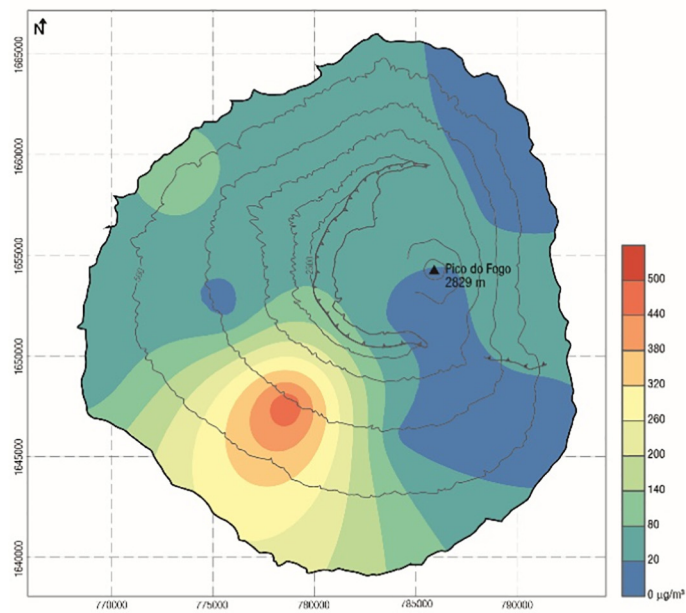


Fig. 7. (continued)

of SO_2 were also below the detection limit, except at Pico Lopes ($85.3 \mu\text{g}/\text{m}^3$). However, contrary to that observed for gaseous pollutants, maximum dust sedimentation rates were not recorded at this site. The fact that biomass combustion mainly generates submicron particles, which present low settling velocities and long residence times that favour their atmospheric dispersion, may explain this finding.

It has been reported that VOCs in fumarolic emissions are dominated by alkanes, alkenes and aromatics (Tassi et al., 2012, 2013, 2015). These hydrocarbons are either formed by metabolic and biosynthetic activity of biological organisms (biogenesis) or by decomposition of pre-existing organic matter occurring at temperatures ($> 150^\circ\text{C}$) too high for bacteria survival (thermogenesis). The dominant VOCs were alkylpentanes, hexane, cycloalkanes and toluene (Fig. 7). The remaining fumarolic activity seems to have little impact on

gaseous air pollution, which is most affected by anthropogenic emission sources. Regardless the location, benzene was always present at concentrations lower than $2 \mu\text{g}/\text{m}^3$, ranging between 0.8 and $1.9 \mu\text{g}/\text{m}^3$. Benzene in ambient air is regulated by the European Union Directive 2008/50/EC (European Commission, 2008), which imposes a mean annual threshold of $5 \mu\text{g}/\text{m}^3$. Ethylbenzene, m,p-xylene and o-xylene peaked at S. Filipe, the capital (location 1), with levels of 10.4, 8.0 and $3.0 \mu\text{g}/\text{m}^3$, respectively. Levels of aromatic compounds are within the range of values reported for various cities worldwide (Table 2). Park et al. (2015) measured the atmospheric concentrations of aromatic hydrocarbons in Deokjeok and Jeju Islands in the Yellow Sea, where no significant emission sources are found. Mean levels of 0.73, 2.49, 0.35, 0.61 and $0.26 \mu\text{g}/\text{m}^3$ were obtained in Deokjeok for benzene, toluene, ethylbenzene, m,p-xylene and o-xylene, respectively. The

Table 2
BTEX levels in ambient air of various cities worldwide ($\mu\text{g}/\text{m}^3$). Values from the literature compiled by Kerchich and Kerbach (2012).

Cities	Benzene	Toluene	Ethylbenzene	m,p-Xylenes	o-Xylene
S. Filipe, this study	1.1	41.8	10.4	8.0	3.0
Algiers, Algeria	1.94	4.57	1.2	1.07	0.55
London, UK	2.7	7.2	1.4	3.7	1.5
Berlin, Germany	6.9	13.8	2.8	7.5	2.9
Rome, Italy	35.5	99.7	17.6	54.1	25.1
Helsinki, Finland	2.1	6.6	1.3	4.1	1.6
Toulouse, France	2	6.6		1.2	3.7
La Coruña, Spain	3.43	23.6	3.34	5.08	2.74
Pamplona, Spain	2.84	13.3	2.15	6.01 ^a	
Bombay, India	13.7	11.1	0.4	1.3	2.2
Guangzhou, Nanhai, and Macau, China	20.0–51.5	39.1–85.9	3.0–24.1	14.2–95.6 ^a	
Seoul, South Korea	3.2	24.5	3.0	10	3.5
São Paulo, Brazil	4.6	44.8	13.3	26.1	6.9
13 sites in 8 states, USA	0.8–3.6	1.5–10.5	0.6–2.4	1.8–5.2	0.6–1.9

^a (m + p + o)-Xylenes.

corresponding concentrations in Jeju were 0.54, 1.73, 0.22, 0.35 and $0.09 \mu\text{g}/\text{m}^3$.

For reasons we do not know, the highest concentrations of several VOCs were registered in Monte Grande (location 5): toluene ($503 \mu\text{g}/\text{m}^3$), 2-methylpentane ($334 \mu\text{g}/\text{m}^3$), 3-methylpentane ($343 \mu\text{g}/\text{m}^3$), hexane ($270 \mu\text{g}/\text{m}^3$), methylcyclopentane ($184 \mu\text{g}/\text{m}^3$), cyclohexane ($27 \mu\text{g}/\text{m}^3$), 2,2-dimethylpentane ($18 \mu\text{g}/\text{m}^3$), 2,4-dimethylpentane ($52 \mu\text{g}/\text{m}^3$), heptane ($2.4 \mu\text{g}/\text{m}^3$), and ethyl acetate ($13 \mu\text{g}/\text{m}^3$). Perhaps the additional anthropogenic activities resulting from resettlement at this village of the populations affected by the eruption may have contributed to enhanced emissions of these compounds. Phenol ($2.3 \mu\text{g}/\text{m}^3$) was only detected at Monte Lantico, a location in the crater of the volcano.

An excellent linear correlation ($r^2 = 0.99$) between m,p-xylene and ethylbenzene was found. It has been reported that their ratios remained relatively constant at different locations in Europe, Asia, and South America because they share common emission sources (Park et al., 2015). The m,p-xylene/ethylbenzene ratio has been also pointed out as an useful tool for estimating the photochemical age of an air mass. In this study, the ratio of m,p-xylene/ethylbenzene determined by the slope of the fitted line was 1.3. This value is within those documented for the remote islands in the Yellow Sea, revealing that air masses arriving at Cape Verde have been subjected to significant aging processes. These compounds are present in relatively constant proportion in the major anthropogenic sources (e.g. vehicle exhaust, refineries, etc.) with ratios in a narrow interval between 2.8 and 4.6 (Monod et al., 2001). However, differences in photochemical reactivity cause the isomers to disappear from the atmosphere at notably different rates. Because of the higher reaction rates with hydroxyl radical (OH \cdot), $18.8 \times 10^{12} \text{ cm}^3/\text{molecule/s}$ for m,p-xylene at 298 K versus $7.1 \text{ cm}^3/\text{molecule/s}$ for ethylbenzene (Atkinson and Arey, 2007; Yu et al., 2015), xylenes have shorter lifetimes. Similarly, toluene has a shorter atmospheric lifetime than benzene due to faster photochemical removal by OH \cdot (rate constants of $5.96 \times$ and $1.23 \times 10^{12} \text{ cm}^3/\text{molecule/s}$ for toluene and benzene, respectively, at 298 K; Atkinson and Arey, 2007; Yu et al., 2015). Thus, the toluene/benzene ratio can also indicate the photochemical age of the pollution carried by air masses. As toluene is more rapidly removed by oxidation, the toluene/benzene ratio gradually decreases as air is transported over longer distances away from the source. Although dependent on the fuel composition, vehicular exhaust emission ratios from combustion during transient engine operation within Europe typically yield ratios in the range from 1.25 and 2.5 ppbv/ppbv, but the introduction of catalytic converters has been shown to significantly decrease the toluene/benzene values (Shaw et al., 2015). Although, as observed for other pollutants, it would be expected that the toluene/benzene ratios revealed aging of the air masses through photochemical processes, the high mean value (~ 22) suggest

that extra sources contribute locally to the toluene levels. It must be borne in mind that the limited car fleet in Fogo is outdated in relation to Europe. Additional sources such as inter-island ferries and cargo ships that dock in the port of São Filipe should be considered. Moreover, toluene is a common solvent for paints, paint thinners, silicone sealants, rubber, printing ink, adhesives (glues), lacquers, disinfectants, etc. It can also be the raw material for polyurethane foams, and is used in the agricultural sector against roundworms and hookworms. Thus, the possible local contribution of some of these sources may override long-distance transport and associated photochemical degradation of toluene.

4. Conclusions

In the absence of regular and continuous air quality monitoring on the Cape Verdean island of Fogo, a screening programme based on passive sampling techniques was established in order to obtain the first overview of the background concentrations and the spatial distribution of some atmospheric pollutants. This study revealed that deposition rates of total settleable dust and its chemical composition are influenced by Saharan desert mineral dust, mixed with industrial emissions, sea salt and biomass burning components. In fact, dust is likely linked to industrial emissions from crude oil refineries, fertiliser industries, as well as oil and coal power plants, located in the northern and north-western coast of the African continent. Smoke plumes from wildfires in western Africa also affect Cape Verde. Moreover, anthropogenic pollution transported by the westerlies, which flow from North America through the North Atlantic at mid- and subtropical latitudes, may contribute to the sulphate, nitrate, ammonium and mineral loads observed in Fogo, although a detailed temporal chemical speciation of settleable dust, combined with high resolution backward air trajectories, would be needed to confirm this assumption. The settleable dust deposition rates are within the ranges reported for other remote locations. The SEM analysis of several particles with different compositions, shapes and sizes revealed high silica mass fractions in all samples, as well as variable contents of carbonates, sulphates, aluminosilicates, Fe, Ti, F and NaCl. The results suggest that these particles have distinct origins, such as volcanic environment, transported Saharan dust, marine salts, organic nature (e.g. bioaerosols), anthropogenic pollution (e.g. biomass burning, urban and industrial emissions), and a mixture of all these sources. Concentrations and ratios between some volatile aromatic hydrocarbons also revealed photochemically processed air masses. The remaining fumarolic activity in Fogo Island seems to have little impact on gaseous air pollution. Some local sources may contribute, however, to relatively high levels of toluene, acid gases and SO_2 in specific sites. Concentrations of benzene were much lower than the threshold stipulated by the European Commission. In most locations,

SO₂ and acid gases were present at undetectable levels.

This screening study has provided valuable input to the design of a more advanced monitoring programme. The location of Cape Verde and the absence of relevant local sources of anthropogenic atmospheric pollutants make this archipelago the ideal place to evaluate the impact of external contributions on the background levels registered over the north-eastern tropical Atlantic.

Acknowledgments

This work was funded by the Portuguese Foundation for Science and Technology (FCT) through the project “Fogo Island volcano: multi-disciplinary Research on 2014 Eruption (FIRE)”, PTDC/GEOGEO/1123/201. Estela Vicente and Carla Candeias acknowledge the FCT scholarships SFRH/BD/117993/2016 and SFRH/BPD/99636/2014, respectively.

Appendix A. Supplementary material

Supplementary data to this article can be found online at <https://doi.org/10.1016/j.atmosres.2018.08.002>.

References

- Almeida-Silva, M., Almeida, S.M., Freitas, M.C., Pio, C.A., Nunes, T., Cardoso, J., 2013. Impact of Sahara dust transport on Cape Verde atmospheric element particles. *J. Toxicol. Env. Heal. A* 76, 240–251.
- Almuhanna, E.A., 2015. Dustfall associated with dust storms in the Al-Ahsa oasis of Saudi Arabia. *Open J. Air Pollut.* 4, 65–75.
- Alves, C., Gonçalves, C., Fernandes, A.P., Tarelho, L., Pio, C., 2011. Fireplace and woodstove fine particle emissions from combustion of western Mediterranean wood types. *Atmos. Res.* 101, 692–700.
- Amodio, M., Catino, S., Dambruoso, P.R., de Gennaro, G., Di Gilio, A., Giungato, P., Laiola, E., Marzocca, A., Mazzone, A., Sardaro, A., Tutino, M., 2014. Atmospheric deposition: sampling procedures, analytical methods, and main recent findings from the scientific literature. *Adv. Meteorol.* 2014, 161730. <https://doi.org/10.1155/2014/161730>.
- Atkinson, R., Arey, J., 2007. Mechanisms of the gas-phase reactions of aromatic hydrocarbons and PAHs with OH and NO₃ radicals. *Polycycl. Aromat. Comp.* 27, 15–40.
- Brooks, N., Chiapello, I., Lerner, S.D., Drake, N., Legrand, M., Moulin, C., Prospero, J., 2005. The climate-environment society nexus in the Sahara from prehistoric times to the present day. *J. North Afr. Stud.* 10, 253–292.
- Calvo, A.I., Alves, C., Castro, A., Pon, V., Vicente, A.M., Fraile, R., 2013. Research on aerosol sources and chemical composition: past, current and emerging issues. *Atmos. Res.* 120–121, 1–28.
- Cao, J., Shen, Z., Chow, J.C., Qi, G., Watson, J.G., Clark, D.R., 2009. Seasonal variations and sources of mass and chemical composition for PM₁₀ aerosol in Hangzhou, China. *Particuology* 7, 161–168.
- Chiapello, I., Bergametti, G., Catenet, B., Bousquet, P., Dulac, F., Santos Soares, E., 1997. Origins of African dust transported over the northeastern tropical Atlantic. *J. Geophys. Res.* 102, 13701–13709.
- Chow, J.C., Watson, J.G., 2002. PM_{2.5} carbonate concentrations at regionally representative Interagency Monitoring of Protected Visual Environment sites. *J. Geophys. Res.* 107 (D21), 8344. <https://doi.org/10.1029/2001JD000574>.
- Clark, D.R., 2013. TANBREEZ Project. Dust Dispersion Study. Tanbreez Mining Greenland A/S. AirQuality.dk, Jyllinge, Denmark.
- Draxler, R.R., Hess, G.D., 1998. Description of the HYSPLIT 4 modeling system, NOAA Tech. Memo. ERL ARL-224. NOAA Air Resources Laboratory, Silver Spring, MD.
- Draxler, R.R., Rolph, G.D., 2003. HYSPLIT (HYbrid Single-Particle Lagrangian Integrated Trajectory) Model access via NOAA ARL READY Website. <http://www.arl.noaa.gov/ready/hysplit4.html> NOAA Air Resources Laboratory, Silver Spring, MD.
- EA, 2013. Technical Guidance Note M17 (Monitoring). Monitoring Particulate Matter in Ambient Air around Waste Facilities. Version 2. Environmental Agency, England.
- European Commission, 2008. Directive 2008/50/EC of the European Parliament and of the Council of 21 May 2008 on Ambient Air Quality and Cleaner Air for Europe. pp. 1–44.
- Fialho, P., Cerqueira, M., Pio, C., Cardoso, J., Nunes, T., Custódio, D., Alves, C., Almeida, S.M., Almeida-Silva, M., Reis, M., Rocha, F., 2014. The application of a multi-wavelength aethalometer to estimate iron dust and black carbon concentrations in the marine boundary layer of Cape Verde. *Atmos. Environ.* 97, 136–143.
- Fomba, K.W., Müller, K., van Pinxteren, D., Herrmann, H., 2013. Aerosol size-resolved trace metal composition in remote northern tropical Atlantic marine environment: case study Cape Verde islands. *Atmos. Chem. Phys.* 13, 4801–4814.
- Fomba, K.W., Müller, K., van Pinxteren, D., Poulain, L., van Pinxteren, M., Herrmann, H., 2014. Long-term chemical characterization of tropical and marine aerosols at the Cape Verde Atmospheric Observatory (CVAO) from 2007 to 2011. *Atmos. Chem. Phys.* 14, 8883–8904.
- Formenti, P., Andreae, M.O., Lange, L., Roberts, G., Cafmeyer, J., Rajta, I., Maenhaut, W., Holben, B.N., Artaxo, P., Lelieveld, J., 2001. Saharan dust in Brazil and Suriname during the Large scale Biosphere–Atmosphere Experiment in Amazonia (LBA)-Cooperative LBA Regional Experiment (CLAIRE) in March 1998. *J. Geophys. Res.* 106 (D14), 14919–14934.
- Formenti, P., Elbert, W., Maenhaut, W., Haywood, J., Andreae, M.O., 2003. Chemical composition of mineral dust aerosol during the Saharan Dust Experiment (SHADE) airborne campaign in the Cape Verde region, September 2000. *J. Geophys. Res.* 108, D18. <https://doi.org/10.1029/2002JD002648>.
- Gaidajis, G., 2002. Deposition rates of total settleable dust and its elemental composition at mountainous background areas in northeastern Chalkidiki, Greece. *J. Environ. Prot. Ecol.* 3, 324–334.
- Gama, C., Tchepel, O., Baldasano, J.M., Basart, S., Ferreira, J., Pio, C., Cardoso, J., Borrego, C., 2015. Seasonal patterns of Saharan dust over Cape Verde - a combined approach using observations and modelling. *Tellus B* 67, 24410. <https://doi.org/10.3402/tellusb.v67.24410>.
- García, M.I., Rodríguez, S., Alastuey, A., 2017. Impact of North America on the aerosol composition in the North Atlantic free troposphere. *Atmos. Chem. Phys.* 17, 7387–7404.
- Gonçalves, C., Alves, C., Nunes, T., Rocha, S., Cardoso, J., Cerqueira, M., Pio, C., Almeida, S.M., Hillamo, R., Teinila, K., 2014. Organic characterisation of PM₁₀ in Cape Verde under Saharan dust influxes. *Atmos. Environ.* 89, 425–432.
- Haywood, J., Francis, P., Osborne, S., Glew, M., Loeb, N., Highwood, E., Tanré, D., Myhre, G., Formenti, P., Hirst, E., 2003. Radiative properties and direct radiative effect of Saharan dust measured by the C-130 aircraft during SHADE: 1. Solar spectrum. *J. Geophys. Res.* 108(D18), 8577. <https://doi.org/10.1029/2002JD002687>.
- Jenkins, G.S., Robjohn, M.L., Demoz, B., Stockwell, W.R., Ndiaye, S.A., Drame, M.S., Gueye, M., Smith, J.W., Luna-Cruz, Y., Clark, J., Holt, J., Paulin, C., Brickhouse, A., Williams, A., Abdullah, A., Reyes, A., Mendes, L., Valentine, A., Camara, M., 2013. Multi-site tropospheric ozone measurements across the north Tropical Atlantic during the summer of 2010. *Atmos. Environ.* 70, 131–148.
- Kerchich, Y., Kerbachi, R., 2012. Measurement of BTEX (benzene, toluene, ethylbenzene, and xylene) levels at urban and semirural areas of Algiers City using passive air samplers. *J. Air Waste Manag. Assoc.* 62, 1370–1379.
- Kerminen, V.M., Hillamo, R., Teinila, K., Pakkanen, T., Allegrini, I., Sparapani, R., 2001. Ion balances of size-resolved tropospheric aerosol samples: implications for the acidity and atmospheric processing of aerosols. *Atmos. Environ.* 35, 5255–5265.
- Kim, B.M., Teffera, S., Zeldin, M.D., 2000. Characterization of PM_{2.5} and PM₁₀ in the South Coast Air Basin of Southern California: part 1 - spatial variations. *J. Air Waste Manag. Assoc.* 50, 2034–2044.
- Krueger, B.J., Grassian, V.H., Cowin, J.P., Laskin, A., 2004. Heterogeneous chemistry of individual mineral dust particles from different dust source regions: the importance of particle mineralogy. *Atmos. Environ.* 38, 6253–6261.
- Laskin, A., Iedema, M.J., Ichkovich, A., Graber, E.R., Taraniuk, I., Rudich, Y., 2005. Direct observation of completely processed calcium carbonate dust particles. *Faraday Disc.* 130, 453–468.
- Molinaroli, E., 1996. Mineralogical characterization of Saharan dust with a view to its final destination in Mediterranean sediments. In: Guerzoni, S., Chester, R. (Eds.), *The impact of Desert dust Across the Mediterranean*. Kluwer Academic Publishers, The Netherlands, pp. 153–162.
- Molinaroli, E., Pistolato, M., Rampazzo, G., Guerzoni, S., 1999. Geochemistry of natural and anthropogenic fall-out (aerosol and precipitation) collected from the NW Mediterranean: two different multivariate statistical approaches. *Appl. Geochem.* 14, 423–432.
- Monod, A., Sive, B.C., Avino, P., Chen, T., Blake, D.R., Rowland, F.S., 2001. Monoaromatic compounds in ambient air of various cities: a focus on correlations between the xylenes and ethylbenzene. *Atmos. Environ.* 35, 135–149.
- Morales-Baquero, R., Pulido-Villena, E., Reche, I., 2013. Chemical signature of Saharan dust on dry and wet atmospheric deposition in the south-western Mediterranean region. *Tellus B* 65, 18720. <https://doi.org/10.3402/tellusb.v65i0.18720>.
- Müller, K., Lehmann, S., van Pinxteren, D., Gnauk, T., Niedermeier, N., Wiedensohler, A., Herrmann, H., 2010. Particle characterization at the Cape Verde atmospheric observatory during the 2007 RHAMBLE intensive. *Atmos. Chem. Phys.* 10, 2709–2721.
- N'Datchoh, E.T., Konaré, A., Diedhiou, A., Diawara, A., Quansah, E., Assamoi, P., 2015. Effects of climate variability on savannah fire regimes in West Africa. *Earth Syst. Dynam.* 6, 161–174.
- Niedermeier, N., Held, A., Müller, T., Heinold, B., Schepanski, K., Tegen, I., Kandler, K., Ebert, M., Weinbruch, S., Read, K., Lee, J., Fomba, K.W., Müller, K., Herrmann, H., Wiedensohler, A., 2014. Mass deposition fluxes of Saharan mineral dust to the tropical northeast Atlantic Ocean: an intercomparison of methods. *Atmos. Chem. Phys.* 14, 2245–2266.
- Pan, X., Uno, I., Wang, Z., Nishizawa, T., Sugimoto, N., Yamamoto, S., Kobayashi, H., Sun, Y., Fu, P., Tang, X., Wang, Z., 2017. Real-time observational evidence of changing Asian dust morphology with the mixing of heavy anthropogenic pollution. Real-time observational evidence of changing Asian dust morphology with the mixing of heavy anthropogenic pollution. *Sci. Rep.* 7, 335. <https://doi.org/10.1038/s41598-017-00444-w>.
- Park, S.M., Kim, J.S., Lee, G., Jang, Y., Lee, M., Kang, C.H., Sunwoo, Y., 2015. Characteristics of the major atmospheric aromatic hydrocarbons in the Yellow Sea. *Asian J. Atmos. Environ.* 9-1, 57–65.
- Patey, M.D., Achterberg, E.P., Rijkenberg, M.J., Pearce, R., 2015. Aerosol time-series measurements over the tropical Northeast Atlantic Ocean: Dust sources, elemental composition and mineralogy. *Mar. Chem.* 174, 103–119.
- Quinn, P.K., Coffman, D.J., Bates, T.S., Miller, T.L., Johnson, J.E., Welton, E.J., Neusüss, C., Miller, M., Sheridan, P.J., 2002. Aerosol optical properties during INDOEX 1999: Means, variability, and controlling factor. *J. Geophys. Res.* 107 (D19), 8020. <https://doi.org/10.1029/2000JD000037>.

- Read, K.A., Carpenter, L.J., Arnold, S.R., Beale, R., Nightingale, P.D., Hopkins, J.R., Lewis, A.C., Lee, J.D., Mendes, L., Pickering, S.J., 2012. Multi-annual observations of acetone, methanol and acetaldehyde in remote tropical Atlantic air: implications for atmospheric OVOC budgets and oxidative capacity. *Environ. Sci. Technol.* 46, 11028–11039.
- Remoundaki, E., Bourliva, A., Kokkalis, P., Mamouri, R.E., Papayannis, A., Grigoratos, T., Samara, C., Tsezos, M., 2011. PM₁₀ composition during an intense Saharan dust transport event over Athens (Greece). *Sci. Total Environ.* 409, 4361–4372.
- Riley, J.P., Chester, R., 1971. *Introduction to Marine Chemistry*. Academic, San Diego, USA.
- Rodríguez, S., Alastuey, A., Alonso-Pérez, S., Querol, X., Cuevas, E., Abreu-Afonso, J., Viana, M., Pérez, N., Pandolfi, M., de la Rosa, J., 2011. Transport of desert dust mixed with North African industrial pollutants in the subtropical Saharan air layer. *Atmos. Chem. Phys.* 11, 6663–6685.
- Salvador, P., Almeida, S.M., Cardoso, J., Almeida-Silva, M., Nunes, T., Cerqueira, M., Alves, C., Reis, M.A., Chaves, P.C., Artiñano, B., Pio, C., 2016. Composition and origin of PM₁₀ in Cape Verde: Characterization of long-range transport episodes. *Atmos. Environ.* 127, 326–339.
- Sander, R., Pszenny, A.A.P., Keene, W.C., Crete, E., Deegan, B., Long, M.S., Maben, J.R., Young, A.H., 2013. Gas phase acid, ammonia and aerosol ionic and trace element concentrations at Cape Verde during the Reactive Halogens in the Marine Boundary Layer (RHAMBLe) 2007 intensive sampling period. *Earth Syst. Sci. Data* 5, 385–392.
- Scheuvs, D., Kandler, K., 2014. On composition, morphology and size distribution of airborne mineral dust. In: Knippertz, P., Stuut, J.B.W. (Eds.), *Mineral Dust - A Key Player in the Earth System*. Springer, Dordrecht, pp. 15–49.
- Scheuvs, D., Schütz, L., Kandler, K., Ebert, M., Weinbruch, S., 2013. Bulk composition of northern African dust and its source sediments - a compilation. *Earth-Sci. Rev.* 116, 170–194.
- Shaw, M.D., Lee, J.D., Davison, B., Vaughan, A., Purvis, R.M., Harvey, A., Lewis, A.C., Hewit, C.N., 2015. Airborne determination of the temporo-spatial distribution of benzene, toluene, nitrogen oxides and ozone in the boundary layer across Greater London, UK. *Atmos. Chem. Phys.* 15, 5083–5097.
- Shi, Z., Zhang, D., Hayashi, M., Ogata, H., Ji, H., Fujie, W., 2008. Influences of sulfate and nitrate on the hygroscopic behaviour of coarse dust particles. *Atmos. Environ.* 42, 822–827.
- Stein, A.F., Draxler, R.R., Rolph, G.D., Stunder, B.J.B., Cohen, M.D., Ngan, F., 2015. NOAA's HYSPLIT Atmospheric transport and dispersion modeling system. *Bull. Am. Meteorol. Soc.* 96, 2059–2077.
- Sullivan, R.C., Moore, M.J.K., Petters, M.D., Kreidenweis, S.M., Roberts, G.C., Prather, K.A., 2009. Effect of chemical mixing state on the hygroscopicity and cloud nucleation properties of calcium mineral dust particles. *Atmos. Chem. Phys.* 9, 3303–3316.
- Tassi, F., Capecciacci, F., Cabassi, J., Calabrese, S., Vaselli, O., Rouwet, D., Pecoraino, G., Chiodini, G., 2012. Geogenic and atmospheric sources for volatile organic compounds in fumarolic emissions from Mt. Etna and Vulcano Island (Sicily, Italy). *J. Geophys. Res.* 117, D17305. <https://doi.org/10.1029/2012JD017642>.
- Tassi, F., Capecciacci, F., Giannini, L., Vougioukalakis, G.E., Vaselli, O., 2013. Volatile organic compounds (VOCs) in air from Nisyros Island (Dodecanese Archipelago, Greece): Natural versus anthropogenic sources. *Environ. Pollut.* 180, 111–121.
- Tassi, F., Venturi, S., Cabassi, J., Capecciacci, F., Nisi, B., Vaselli, O., 2015. Volatile organic compounds (VOCs) in soil gases from Solfatara crater (Campi Flegrei, southern Italy): Geogenic source(s) vs. biogeochemical processes. *Appl. Geochem.* 56, 37–49.
- Terzi, E., Argyropoulos, G., Bougatioti, A., Mihalopoulos, N., Nikolaou, K., Samara, C., 2010. Chemical composition and mass closure of ambient PM₁₀ at urban sites. *Atmos. Environ.* 44, 2231–2239.
- Weinzierl, B., Sauer, D., Esselborn, M., Petzold, A., Veira, A., Rose, M., Mund, S., Wirth, M., Ansmann, A., Tesche, M., Gross, S., Freudenthaler, V., 2011. Microphysical and optical properties of dust and tropical biomass burning aerosol layers in the Cape Verde region - an overview of the airborne in situ and Lidar measurements during SAMUM-2. *Tellus B* 63, 589–618.
- Yu, X., Deng, J., Yi, B., Liu, W., 2015. Predicting rate constants of hydroxyl radical reactions with alkenes and aromatics. *J. Atmos. Chem.* 72, 29–141.